CHIN. PHYS. LETT. Vol. 38, No. 8 (2021) 084201

Towards High-Dimensional Entanglement in Path: Photon-Source Produced from a Two-Dimensional Atomic Cloud

Shaoxing Liu(刘少星)[1], Xuanying Lai(赖宣颖)[1], Ce Yang(杨策)[1], and J. F. Chen(陈洁菲)[1,2*]

[1]*State Key Laboratory of Precision Spectroscopy, School of Physics and Electronic Science, East China Normal University, Shanghai 200241, China*

[2]*Shenzhen Institute for Quantum Science and Engineering and Department of Physics, Southern University of Science and Technology, Shenzhen 518055, China*

(Received 18 March 2021; accepted 21 May 2021; published online 2 August 2021)

A photon source with high-dimensional entanglement is able to bring increasing capacity of information in quantum communication. The dimensionality is determined by the chosen degree of freedom of the photons and is limited by the complexity of the physical systems. Here we propose a new type of high-dimensional entangled photon source, generated via path-indistinguishable scheme from a two-dimensional atomic cloud, which is prepared in a magneto-optical trap. To verify the photon source, we demonstrate experimentally the quantum state of the single photons heralded by its partner photon, with homodyne tomographic technology.

DOI: 10.1088/0256-307X/38/8/084201

High-dimensional photonic quantum states offer great advantages for quantum communication, such as higher information capacity, resistance to noise in quantum key distribution, and they are a better shaper than qubits in local realism and quantum mechanics testing.[1−4] Photons have quite a few choices of degrees of freedom (DoF) to encode high-dimensional quantum information, including orbital angular momentum (OAM),[5,6] discrete time bin and frequency bin.[7] However, manipulation of OAM in high-dimensional space is hard to be realized.[8] In addition, long-distance communication with this DoF through fibers is still the main challenge.[9] High-dimensional time-bin qudits usually require imbalance interferometry setup and phase locking technology, although recent reports demonstrate that the time and frequency domain can be well manipulated through ultra-fast optical pulse reshaping.[10,11] Path DoF is also well developed in SPDC community,[12] and manipulation of this type of qudit has been demonstrated using beam splitters and phase shifters.[13]

The most accessible high-dimensional entangled states can be generated from photon pairs via two approaches: spontaneous parametric down conversion (SPDC) in a nonlinear crystal[14−17] and spontaneous four-wave mixing (SFWM) in an atomic ensemble.[18,19] An ultra-fast pump laser pulse focused into a specific spot in the crystal can excite paired photons in this $\chi^{(2)}$ medium.[20,21] Due to the wide-band feature, produced paired photons are almost simultaneously emitted with femto-seconds of coherence time. Excited by a coherently split pump beam that focuses on multiports in the crystal, with all other DoFs indistinguishable, the photon pairs generated from N paths become the path entangled paired photons.[22−24] In contrast, atomic ensemble serves as a $\chi^{(3)}$ nonlinear medium,[25,26] the dephasing rates of the atomic states are comparable or much smaller than the atomic natural linewidth, i.e., linewidth of MHz.[27] Furthermore, with the electromagnetically induced transparency (EIT) effect,[28] the biphotons generated from SFWM in two-dimensional cold atomic ensembles have a coherence time exceeding 1 μs.[29,30] The temporal waveform of the paired photons ascribed to the slow light effect of the EIT three-level atomic system.[31,32] The linear susceptibility of the Stokes and anti-Stokes photons greatly differs, i.e., the Stokes photons propagate almost with the speed of light in vacuum (c) and the anti-Stokes photons propagate with a slow light velocity $V_{\rm g}$. The generation location within the long cigarette-shape atomic cloud is random, and each location corresponding to different arrival time of the anti-Stokes photons. Therefore, the path information of the photon source is transformed to time-bin information, which is determined by identifying the relative delay time of anti-Stokes photons with respect to their individual partner photons. In this case, the path entanglement of the photons generated from the two-dimensional cold atomic cloud is equivalent to the time-bin entanglement.[33,34]

Supported by the National Natural Science Foundation of China (Grant No. 12074171), the Guangdong Key Project (Grant No. 2019ZT08X324), the Guangdong Innovation Project (Grant No. 2019KTSCX160), and Guangdong Provincial Key Laboratory (Grant No. 2019B121203002).

*Corresponding author. Email: jfchen@phy.ecnu.edu.cn

© 2021 Chinese Physical Society and IOP Publishing Ltd

Although the paired photons generated from this two-dimensional atomic system are widely discussed, the potential configuration for emitting path entangled photon pairs is not yet discussed. In particular, the quantum state of the paired photons emitted is worthy of further verification. In contrast from the conventional photon counting scheme to characterize this photonic quantum source, in this Letter we utilize the balanced homodyne detection (BHD) scheme[35] to reconstruct the reduced quantum state of the paired photons with one of the photons as the trigger. The mode-matching between the local oscillator (LO) in BHD and the target photons is improved compared to the previous experimental setup[36] by splitting part of the LO beam and shifting its frequency over 3 GHz by an electric-optic modulator to provide the coupling beam in SFWM. Therefore, within the photon source, we obtain more than 29% for the single-photon-composition, with the coherence time exceeding 200 ns.

We use a pair of counter-propagating pump beams to excite the SFWM in the 2D atomic cloud with length L. According to the phase-matching condition, the generated Stokes and anti-Stokes photons propagate along the opposite direction respect to each other. As shown in Fig. 1, we cut the whole atomic cloud into N slices, and in each slice we assume that there are an infinitesimal number of atoms located in the region. Furthermore, if the two pump beams of the SFWM process cover the whole atomic cloud perfectly, then the nonlinear coupling coefficients for the paired photons are uniform along the whole length L. With the same uniform excitation configuration, the linear susceptibility of the Stokes or anti-Stokes photon is again uniform along the cloud. This guarantees that wherever the paired photons generate, they propagate through the cloud with the same dispersion. With the assumption that the paired photons are generated at slices 1, 2, to N with equal probability, the path entangled state of paired photons can be expressed as

$$|\Psi\rangle_{\text{path}} = \frac{1}{\sqrt{N}}(|1_1, 1_1\rangle + |1_2, 1_2\rangle + \cdots + |1_i, 1_i\rangle + \cdots + |1_N, 1_N\rangle). \quad (1)$$

With all the other DoF being identical (e.g., polarization, propagation vector and spectral distribution), the generation location of these paired photons will be distinguished according to their relative arrival time. Imagine that the cloud is dense enough to make every emitted anti-Stokes photon experience a slow velocity V_g within the EIT dispersion, but keep the Stokes photons propagating with the speed of light in vacuum, c, by far-detuned pumping. The anti-Stokes photons emitted by slice N will arrive with relative delay time $\tau = 0$ because the anti-Stokes photons in this slice immediately exit the cloud and propagate with c. Here we ignore the delay time given by L/c. With the opposite extreme, the anti-Stokes photons emitted by slice 1 arrive with the largest delay time $\tau = L/V_g$. With the Stokes photons as the trigger, the anti-Stokes photons are heralded as single-photon state. Through measuring the photo-current $i(\tau)$ of this single-photon state and integrating over an appropriate temporal mode function $\varphi(\tau)$, we obtain the quadrature amplitude $X = \int i(\tau)\varphi(\tau)d\tau$ and thus the Wigner function to characterize the quantum state of the photon source from this 2D atomic ensemble.

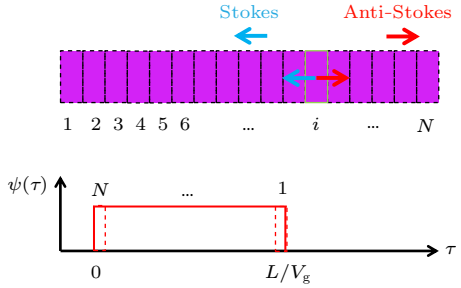

Fig. 1. Generation scheme of path entangled paired photons in two-dimensional atomic cloud. The Stokes and anti-Stokes photons are spontaneously emitted from an atom located in the atomic ensemble, and counter-propagate through the ensemble. Here $\psi(\tau)$ denotes the temporal waveform of the paired photons, with delay time τ denoting the relative arrival time of anti-Stokes photons respect to Stokes photons.

The 2D cold atomic ensemble is prepared with a cloud of cold ^{85}Rb atoms in a magneto-optical trap (MOT). A pump laser beam with a wavelength of 780 nm, which is blue-detuned to the transition $|1\rangle \rightarrow |4\rangle$ by $\Delta_p = 146$ MHz, and a strong coupling laser beam with wavelength of 795 nm, which is resonant to the transition $|2\rangle \rightarrow |3\rangle$, establish the SFWM process. According to the energy level scheme shown in Fig. 2, Stokes and anti-Stokes photons are generated in this parametric process. If we arrange the pump and coupling beam in the SFWM as shown in the figure, then the Stokes and anti-Stokes photons counter-propagate along the direction of the longitudinal axis of the 2D atomic cloud. To avoid scattering noise from the pump and coupling beam, we align them in a direction deviated by 2° from the longitudinal axis. The pump and coupling beams have orthogonal circular polarization and we collect the Stokes and anti-Stokes photons in a specific pair of orthogonal circular polarization, which are selected by a quarter wave plate (QWP1 and QWP2) and a polarization beam splitter (PBS1 and PBS2) as indicated. To excite the whole atomic cloud, the Gaussian beam waist of the pump and coupling beam is 1.6 mm. The Stokes photons are collected through the single-mode fiber (SMF1) by the single-photon counting module (SPCM1). A flipped mirror (M1) is inserted in the receiving end of the anti-Stokes beam to switch the detection scheme from

coincidence counting to BHD. The coherence time can be adjusted from 140 ns to 300 ns by changing the coupling laser power at a certain atomic optical depth (OD).

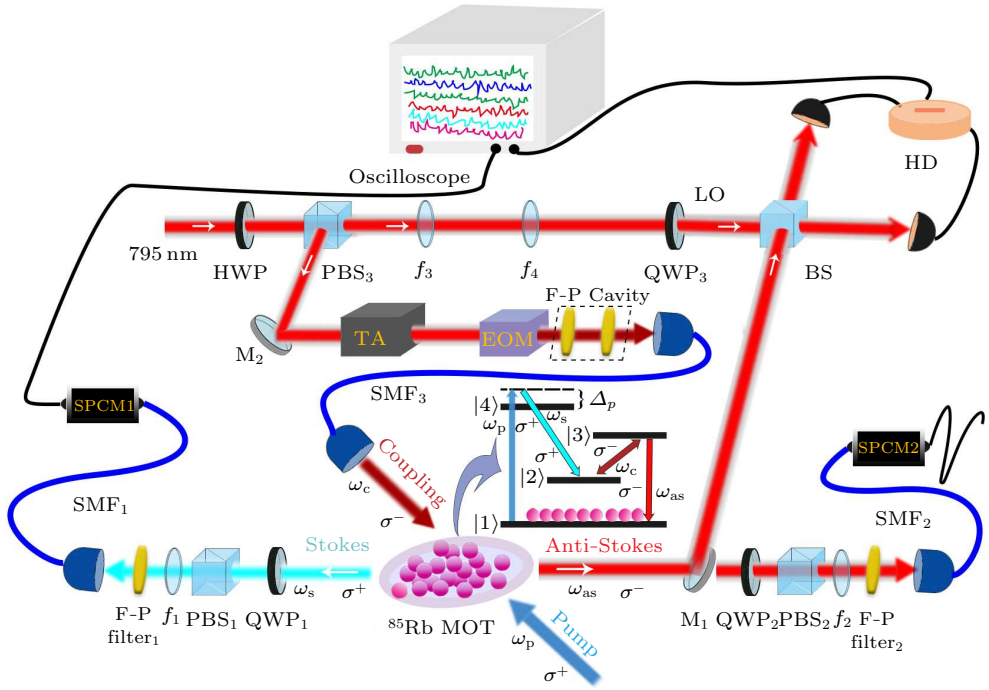

Fig. 2. Experimental setup for the photon pairs generation and homodyne detection measurement. A pair of photons (Stokes and anti-Stokes) are generated from SFWM progress in ^{85}Rb cold atomic ensemble in opposite directions. A continuous 795 nm laser is divided into two parts by a polarized beam splitter (PBS3). One of the beams is amplified by a tapered amplifier (TA) and is further shifted 3.036 GHz by an EOM. The other beam is utilized as the local oscillator (LO), mixed with the anti-Stokes beam at a beam splitter (BS). SFWM: spontaneous four-wave mixing. SPDC: single-photon counting module. BHD: balanced homodyne detector. In the double-Λ energy level scheme, $|1\rangle = 5S_{1/2}$, $F = 2$, $|2\rangle = 5S_{1/2}$, $F = 3$, $|3\rangle = 5P_{1/2}$, $F = 3$ and $|4\rangle = 5P_{3/2}$, $F = 3$. The coupling laser beam is resonant to the transition $|2\rangle \rightarrow |3\rangle$.

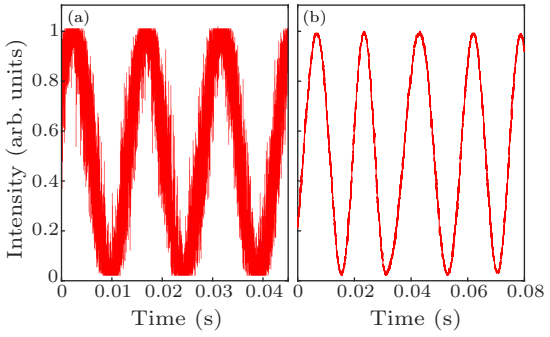

Fig. 3. Interference between the LO beam and the coupling beam of SFWM. (a) The LO beam and the coupling beam are beat locked with frequency difference set as 100 Hz. (b) The LO beam and the coupling beam are from the same laser source.

In the BHD, we need a phase locked laser beam with stable power output to serve as the local oscillator (LO) in the measurement. Ideally, the LO beam should be identical with the anti-Stokes beam generated from the cloud. Instead of using a phase locked beam beat with the coupling beam, we split a part of power of a single stable laser beam for the coupling beam and the remaining power as the LO. Considering that the coupling beam is shifted 3.036 GHz from the anti-Stokes beam, i.e., the LO beam. We use an electro-optical modulator (EOM) to modulate the laser beam (whose power is amplified through a tapered amplifier) and use the sideband as the coupling beam. A pair of Fabry–Pérot etalons which combine to have more than 35 dB in series and with transmission bandwidth of 500 MHz, is located after the EOM to filter its zeroth-order and unwanted sideband. A comparison between the interference between the LO and the anti-Stokes beam is shown in Fig. 3. To obtain the interference shown in Fig. 3(a), we use a laser beam phase-locked with the LO laser to mimic the anti-Stokes photons generated from SFWM. Due to the sideband noise (∼1 MHz) from the locking electronics with phase lock loop scheme, the interference curve exhibits heavy fluctuation with corresponding frequency. In contrast, if we generate the anti-Stokes beam from the same laser beam of the LO field, a clean interference curve showing the mode-matching between the anti-Stokes beam and the LO beam is observed. The interference visibility is up to $v = 0.95 \pm 0.01$ in Fig. 3(b). By reducing the phase noise of the LO relative to the target field, we are able to characterize a photo-current signal approach-

ing 1 μs.

Figures 4(a1), 4(b1) and 4(c1) show the coincidence counts of the paired photons, which indicate $|\varphi(\tau)|^2$, with various power for the coupling and pump beam in SFWM. From Figs. 4(a1)–4(c1), we reduce the coupling beam power to maximize the slow light effect of EIT and thus the coherence time of photon source can be adjusted as 140 ns, 200 ns and 300 ns, respectively. With the coupling beam originated from the same laser source with the LO beam, we obtain the variance of the quadrature amplitude $\langle\Delta^2 X\rangle$ as shown in Figs. 4(a2), 4(b2) and 4(c2), and therefore the quadrature probability distribution $\Pr(X)$ as shown in Figs. 4(a3), 4(b3) and 4(c3). Through the maximum-likelihood method, the corresponding density matrix of the photon source with the Stokes photons as trigger is obtained. The diagonal elements of the density matrix ρ_{nn} are (a) $\rho_{00} = 0.784$, $\rho_{11} = 0.188$ and $\rho_{22} = 0.026$; (b) $\rho_{00} = 0.736$, $\rho_{11} = 0.205$ and $\rho_{22} = 0.039$; (c) $\rho_{00} = 0.804$, $\rho_{11} = 0.180$ and $\rho_{22} = 0.008$. If we consider the non-unity measurement efficiency $\mu = 0.7$, which includes the optical transmission, mode matching between LO and anti-Stokes beam, quantum efficiency and electronic noise of the photo-detector in the BHD setting, μ corrects the density matrix as $\hat{\rho}_{\rm cor} = \frac{\hat{\rho}}{\mu} - \frac{1-\mu}{\mu}|0\rangle\langle 0|$. Figures 4(a3), 4(b3) and 4(c3) calculate the corrected Wigner function according to Wigner's legendary formula.[35] The Wigner function shows the quasi-probability distribution function of the single-photon state, which deviates from the Gaussian behavior.[37–39] Especially, Fig. 4(b3) shows that $W(0,0)$ is lower than the surrounding values. With appropriate pump and coupling beam setting, for the first time we shows a non-Gaussian state for the photon source with coherence time up to 200 ns, as shown in Fig. 4(b2), corresponding to more than 29% for the single-photon composition. The results show that ρ_{22} is slightly larger than a coherent state with the same average photon number. The reason is that the amplified coupling beam of the SFWM process is scattered by the atoms into the BHD detector. To solve this technical problem, one should replace a Fabry-Pérot etalon of high isolation (>40 dB) after the EOM to avoid the unfiltered photons with the frequency of the LO beam.

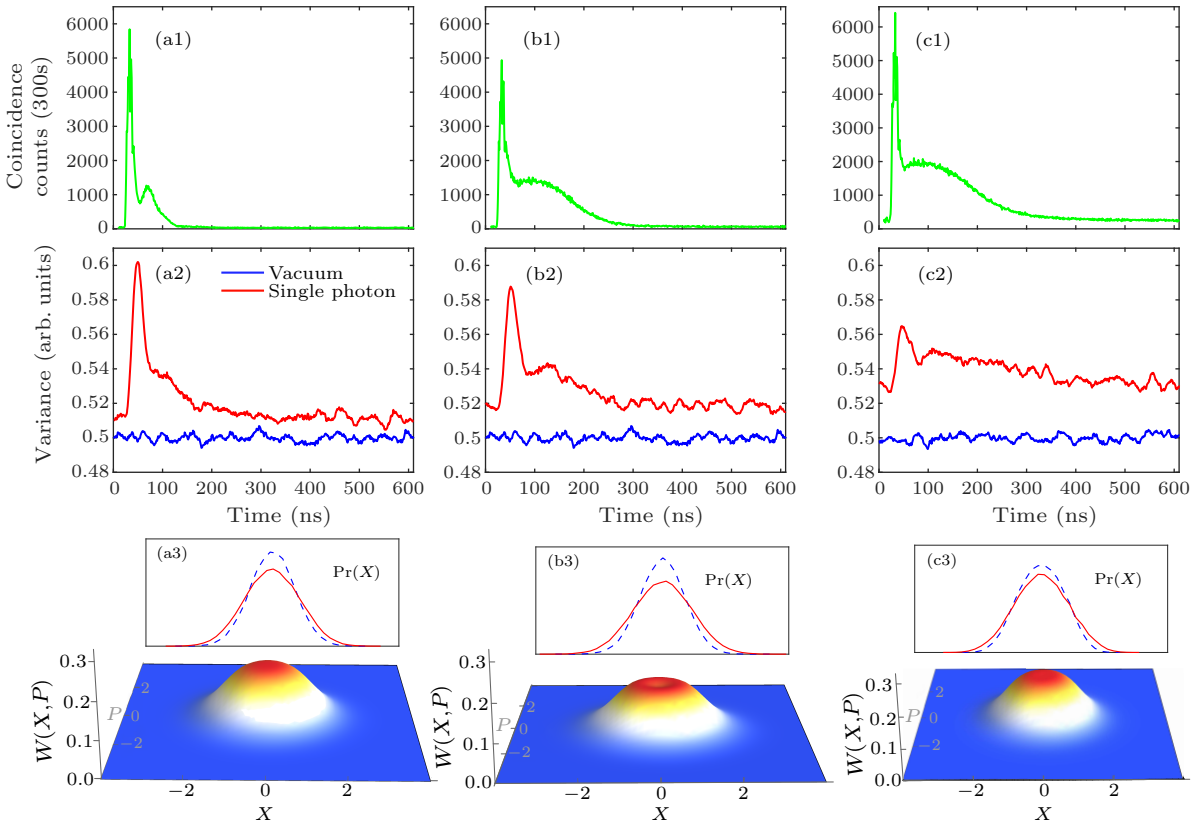

Fig. 4. Characterization of the temporal mode through photon counting and BHD. [(a1), (b1), (c1)] The accumulated coincidence counts of 300 s with different experimental parameters. [(a2), (b2), (c2)] The corresponding variance of quadrature amplitude. The blue solid lines describe the variance of the vacuum state, the red solid line describes the variance of the single photons. The results are accumulated after 10^5 records of the photocurrent data. [(a3), (b3), (c3)] The quadrature probability distribution and the corrected Wigner function. The solid red line represents $\Pr(X)$ of the target state and the blue dotted line represents $\Pr(X)$ of the vacuum state. [(a1), (a2), (a3)] The pump laser power $P_{\rm p} = 100\,\mu$W, coupling laser power $P_{\rm c} = 4.5$ mW, and OD is 60. [(b1), (b2), (b3)] $P_{\rm p} = 100\,\mu$W, coupling laser power $P_{\rm c} = 2$ mW, with OD being 60. [(c1), (c2), (c3)] $P_{\rm p} = 300\,\mu$W, coupling laser power $P_{\rm c} = 1.9$ mW, with OD being 65.

The heralded single photons generated from the 2D atomic cloud demonstrate as non-classical according to the reconstructed Wigner function. The Wigner function deviates from that of an ideal single-photon source because the vacuum state $|0\rangle$ occupies the largest part in the source. The vacuum composition ρ_{00} is much higher than ρ_{11} because of low pairing efficiency in our experimental system. One of the possible cause for a low pairing efficiency is the excitation of the atoms by the pump beam produce excess Stokes photons. The SFWM in the atomic ensemble occurs, accompanied with Raman scattering photons which have the same central frequency of Stokes photons but larger frequency spread. We therefore reduce the Raman scattering noise within the Stokes photons using a narrower Fabry-Pérot filter with linewidth of 70 MHz. Compared to the pairing efficiency 11.7% obtained from the Stokes photons filtered by Fabry-Pérot etalon with 500 MHz, after decreasing the Raman scattering noise the pairing efficiency slightly increases to 12.8%. This is not the main reason for the low efficiency of pairing. Therefore, we conclude that the main reason for the low pairing efficiency is that the collection system suffers from high loss.

In conclusion, we utilize the balanced homodyne detection scheme to reconstruct the reduced quantum state of the paired photons with one of the photons as the trigger. With the LO beam and coupling beam sharing the same laser source, for the first time we show a non-Gaussian state for the photon source with coherence time up to 200 ns. The paired photons are produced by the SFWM process occurring in random location in the 2D cold atomic cloud. Born in different locations of the cloud, the anti-Stokes photons propagate with a slow velocity due to EIT effect within the medium and arrive at different delay times respect to the Stokes photons which always propagate with the speed of light in vacuum. We demonstrate that with up to hundreds of nanoseconds of delay time, the anti-Stokes photons heralded by the Stokes photons still exhibit the nonclassical property. The dispersion caused by the EIT effect therefore preserves the quantum state of the photon source and, more importantly, transforms the degree of freedom of path to time. With improved collection efficiency and manipulation of the atomic cloud, we expect that the photon source generated in this 2D atomic cloud will be able to encode controllable path entanglement.[24]

References

[1] Bechmann-Pasquinucci H and Peres A 2000 *Phys. Rev. Lett.* **85** 3313
[2] Cerf N J, Bourennane M, Karlsson A and Gisin N 2002 *Phys. Rev. Lett.* **88** 127902
[3] Kaszlikowski D, Gnaciński P, Żukowski M, Miklaszewski W and Zeilinger A 2000 *Phys. Rev. Lett.* **85** 4418
[4] Vértesi T, Pironio S and Brunner N 2010 *Phys. Rev. Lett.* **104** 060401
[5] Mair A, Vaziri A, Weihs G and Zeilinger A 2001 *Nature* **412** 313
[6] Erhard M, Fickler R, Krenn M and Zeilinger A 2018 *Light Sci. Appl.* **7** 17146
[7] Brendel J, Gisin N, Tittel W and Zbinden H 1999 *Phys. Rev. Lett.* **82** 2594
[8] Erhard M, Krenn M and Zeilinger A 2020 *Nat. Rev. Phys.* **2** 365
[9] Cozzolino D *et al.* 2019 *Phys. Rev. Appl.* **11** 064058
[10] MacLean J P W, Donohue J M and Resch K J 2018 *Phys. Rev. Lett.* **120** 053601
[11] Donohue J M, Agnew M, Lavoie J and Resch K J 2013 *Phys. Rev. Lett.* **111** 153602
[12] O'Sullivan-Hale M N, Khan I A, Boyd R W and Howell J C 2005 *Phys. Rev. Lett.* **94** 220501
[13] Qiang X *et al.* 2018 *Nat. Photon.* **12** 534
[14] Kaneda F, Suzuki H, Shimizu R and Edamatsu K 2019 *Opt. Express* **27** 1416
[15] Edgar M P *et al.* 2012 *Nat. Commun.* **3** 984
[16] Trajtenberg-Mills S, Karnieli A, Voloch-Bloch N, Megidish E, Eisenberg H S and Arie A 2020 *Laser Photon. Rev.* **14** 1900321
[17] Thyagarajan K *et al.* 2009 *Phys. Rev. A* **80** 052321
[18] Srivathsan B, Gulati G K, Chng B, Maslennikov G, Matsukevich D and Kurtsiefer C 2013 *Phys. Rev. Lett.* **111** 123602
[19] Wang C, Lee C H, Kim Y and Kim Y H 2020 *Opt. Lett.* **45** 1802
[20] Sansoni L, Sciarrino F, Vallone G, Mataloni P, Crespi A, Ramponi R and Osellame R 2010 *Phys. Rev. Lett.* **105** 200503
[21] Zhukovsky S V, Helt L G, Kang D, Abolghasem P, Helmy A S and Sipe J E 2012 *Phys. Rev. A* **85** 013838
[22] Schaeff C *et al.* 2012 *Opt. Express* **20** 16145
[23] Hu X M *et al.* 2016 *Phys. Rev. Lett.* **117** 170403
[24] Li L *et al.* 2020 *Science* **368** 1487
[25] Ding D S, Zhou Z Y, Shi B S and Guo G C 2013 *Nat. Commun.* **4** 2527
[26] Kolchin P, Du S, Belthangady C, Yin G Y and Harris S E 2006 *Phys. Rev. Lett.* **97** 113602
[27] Liao K, Yan H, He J, Du S, Zhang Z M and Zhu S L 2014 *Phys. Rev. Lett.* **112** 243602
[28] Boller K J, Imamoğlu A and Harris S E 1991 *Phys. Rev. Lett.* **66** 2593
[29] Zhao L W, Guo X X, Liu C, Sun Y, Loy M M T and Du S W 2014 *Optical* **1** 84
[30] Han Z G, Qian P, Zhou L, Chen J F and Zhang W 2015 *Sci. Rep.* **5** 9126
[31] Qian P, Gu Z, Cao R, Wen R, Ou Z Y, Chen J F and Zhang W 2016 *Phys. Rev. Lett.* **117** 013602
[32] Yang C, Gu Z, Chen P, Qin Z, Chen J F and Zhang W 2018 *Phys. Rev. Appl.* **10** 054011
[33] Yan H, Zhu S L and Du S W 2011 *Chin. Phys. Lett.* **28** 070307
[34] Liu C *et al.* 2013 *Opt. Express* **21** 9505
[35] Leonhardt U 1997 *Measuring the Quantum State of Light* (Cambridge: Cambridge University Press) p 87
[36] Gu Z, Yang C and Chen J F 2019 *Opt. Commun.* **439** 206
[37] Ariano G and Rasetti M 1987 *Phys. Rev. D* **35** 1239
[38] Straka I *et al.* 2014 *Phys. Rev. Lett.* **113** 223603
[39] Ježek M, Straka I, Mičuda M, Dušek M, Fiurášek J and Filip R 2011 *Phys. Rev. Lett.* **107** 213602